

31. I. Prost *et al.*, *Plant Physiol.* **139**, 1902 (2005).  
 32. Supported by the Max Planck Society. We thank M. Kant, R. Schuurink, E. Gaquerel, G. Bonaventure, and three anonymous reviewers for comments on the manuscript; S. Meldau for providing *ir-sipk* × *ir-wipk* seeds; D. Kessler and C. Diezel for help with the field experiments and enzyme assays; M. Kallenbach and

A. Weinhold for analytical help; and Brigham Young University for the use of their Lytle Ranch Preserve field station.

#### Supporting Online Material

www.sciencemag.org/cgi/content/full/329/5995/1075/DC1  
 Materials and Methods

SOM Text  
 Figs. S1 to S13  
 Tables S1 to S6  
 References

29 April 2010; accepted 13 July 2010  
 10.1126/science.1191634

# Substrate Elasticity Regulates Skeletal Muscle Stem Cell Self-Renewal in Culture

P. M. Gilbert,<sup>1\*</sup> K. L. Havenstrite,<sup>1,2\*</sup> K. E. G. Magnusson,<sup>1,3</sup> A. Sacco,<sup>1†</sup> N. A. Leonardi,<sup>1,4</sup> P. Kraft,<sup>1</sup> N. K. Nguyen,<sup>1</sup> S. Thrun,<sup>5</sup> M. P. Lutolf,<sup>4</sup> H. M. Blau<sup>1‡</sup>

Stem cells that naturally reside in adult tissues, such as muscle stem cells (MuSCs), exhibit robust regenerative capacity in vivo that is rapidly lost in culture. Using a bioengineered substrate to recapitulate key biophysical and biochemical niche features in conjunction with a highly automated single-cell tracking algorithm, we show that substrate elasticity is a potent regulator of MuSC fate in culture. Unlike MuSCs on rigid plastic dishes (~10<sup>6</sup> kilopascals), MuSCs cultured on soft hydrogel substrates that mimic the elasticity of muscle (12 kilopascals) self-renew in vitro and contribute extensively to muscle regeneration when subsequently transplanted into mice and assayed histologically and quantitatively by noninvasive bioluminescence imaging. Our studies provide novel evidence that by recapitulating physiological tissue rigidity, propagation of adult muscle stem cells is possible, enabling future cell-based therapies for muscle-wasting diseases.

Many adult tissues harbor stem cells with a defined identity and marked regenerative capacity. This property is retained if stem cells are immediately transplanted from one individual to another following isolation, but it is lost as soon as the stem cells are plated in culture in order to increase their numbers for therapeutic applications. The muscle microenvironment (niche) enables freshly isolated muscle stem cells (MuSCs) to contribute extensively to skeletal muscle regeneration when transplanted in mice (1–8). In contrast, muscle stem cells grown on standard tissue culture plastic lose “stemness,” yielding progenitors with greatly diminished regenerative potential (3, 7, 9) and therapeutic potency (10). Indeed, the propagation of functional adult stem cells, including MuSCs, is currently not possible in culture, despite extensive research on biochemical signals. Biophysical properties such as matrix rigidity are known to alter the

differentiation of cells in culture (11). Here, we test the hypothesis that the elastic modulus plays a crucial role in muscle stem cell self-renewal and function in muscle regeneration. We report that when MuSCs are cultured on a substrate that mimics the rigidity of muscle tissue, they self-renew to generate stem cell progeny that can potentially repair damaged muscle, establishing a paradigm for overcoming a major roadblock to adult stem cell therapeutic utility. In contrast to induced pluripotent stem (iPS) or embryonic stem cells whose differentiation must be directed, this strategy capitalizes on the existence of native tissue stem cells with defined identities and functions.

To recapitulate muscle rigidity and uncouple biophysical from biochemical effects, we engineered a tunable polyethylene glycol (PEG) hydrogel platform. By altering the percentage of PEG polymer in the precursor solution we produced hydrogels with a range of rigidities (Fig. 1, A and B, top) including a formulation that mimics the elastic modulus of adult murine skeletal muscle (Fig. 1, A and C) (12). Notably, polystyrene plastic traditionally used for cell culture, has an elastic modulus of ~3 GPa, more than five orders of magnitude stiffer than skeletal muscle (13). Laminin, a component of the native MuSC niche, was covalently cross-linked to the hydrogel network and used as an adhesion ligand (Fig. 1B, bottom). To ensure that laminin density and surface chemistry remained consistent between hydrogel and plastic culture conditions, we generated gels that do not swell after polymerization (Fig. 1D and fig. S1) and cast a thin layer of PEG hydrogel (≤1 μm) on the plastic surface, allowing MuSCs to sense

the stiffness of the plastic beneath [see supporting online material (SOM)] (Fig. 1D) (12).

MuSCs were prospectively isolated (7) and analyzed at the single-cell level on pliant or stiff culture surfaces patterned with arrays of microwells (Fig. 1E) (14), because even when enriched by fluorescence-activated cell sorting, stem cell populations are inherently heterogeneous (4, 6–8, 14, 15). Time-lapse acquisition of hundreds of single stem cells is possible using microwell technology (14); however, analysis of the resulting immense data sets remains a major challenge. To enable rapid analysis, we developed a highly automated algorithm termed the Baxter algorithm (SOM), which, in contrast to most commercially available software, is able to track lineage relationships over multiple cell divisions. This algorithm reduced data analysis time by ~90% with a mere 1% error rate.

The genealogic history of clones derived from a single cell was established by time-lapse acquisition and automated tracking (Fig. 1E and movie S1). MuSC velocity increased on stiff (120 μm/hour) compared with pliant (99 μm/hour) culture substrates (Fig. 1F, *P* < 0.0001), in agreement with previous reports investigating cell lines (16). In addition, we observe that cell area increases as cells duplicate their content, returning to initial cell area after mitosis, further validating our segmentation parameters (fig. S2).

MuSCs propagated on pliant hydrogel substrates do not undergo the “crisis,” or massive cell death, previously reported in culture (9, 17). After 1 week of culture in soft microwells, twice as many cells give rise to clones as compared with cells cultured in rigid microwells (fig. S3). Using the Baxter algorithm, we characterized this phenomenon at the clonal level. On rigid substrates, the overall cell number does not change over time because division is offset by death; however, on pliant substrates death is reduced and the total number of cells increases over time (Fig. 1G and figs. S4 and S5). In both conditions, death is not sudden; indeed, it is independent of time and cell division number (Fig. 1G and fig. S4). This data demonstrates that culture on soft substrates augments MuSC survival.

Substrate rigidity also impacts gene expression, suggesting that MuSC stemness is retained on soft surfaces. MuSCs cultured for 1 week on soft substrates give rise to one-third as many cells that express myogenin, a myogenic transcription factor expressed by differentiated MuSCs, than MuSCs cultured on rigid substrates (fig. S6). Time-lapse analysis excludes the possibility that gene expression differences are due to differences in cell division, because we observe no statistically significant difference in MuSC time to first

<sup>1</sup>Baxter Laboratory for Stem Cell Biology, Department of Microbiology and Immunology, Institute for Stem Cell Biology and Regenerative Medicine, Stanford University School of Medicine, Stanford, CA 94305, USA. <sup>2</sup>Department of Chemical Engineering, Stanford University, Stanford, CA 94305, USA. <sup>3</sup>School of Electrical Engineering, Signal Processing Lab, Royal Institute of Technology (KTH), SE-100 44 Stockholm, Sweden. <sup>4</sup>Institute of Bioengineering and Laboratory of Stem Cell Bioengineering, Ecole Polytechnique Fédérale de Lausanne (EPFL), CH-1015 Lausanne, Switzerland. <sup>5</sup>Stanford Artificial Intelligence Lab, Department of Computer Science, Stanford, CA 94305, USA.

\*These authors contributed equally to this work.

†Present address: Sanford-Burnham Medical Research Institute, La Jolla, CA 92037, USA.

‡To whom correspondence should be addressed. E-mail: hblau@stanford.edu

division (fig. S7) or time between divisions (fig. S8). In addition, division rate is not different on pliant compared with rigid substrates (fig. S9 and SOM). These *in vitro* studies demonstrate that

substrate rigidity has no effect on cell division rate in culture but likely prevents differentiation and leads to increased cell numbers by enhancing viability.

To establish definitively that MuSCs cultured on pliant substrates retain stemness, their function was assessed *in vivo*. MuSCs were isolated from mice constitutively expressing firefly lucifer-

**Fig. 1.** Pliant hydrogel promotes MuSC survival and prevents differentiation in culture. **(A)** PEG hydrogels with tunable mechanical properties. Young's modulus ( $E$ ) is linearly correlated with precursor polymer concentration ( $n = 4$ ); red circle indicates muscle elasticity. **(B)** Image of a pliant PEG hydrogel on a green spatula. Scale bar, 7 mm (top). Confocal immunofluorescence image of hydrogel microcontact printed with laminin specifically at the bottom of hydrogel microwells (i.e., from the "tips" of the micropillars). Scale bar, 125  $\mu\text{m}$  (bottom). **(C)** Dissected tibialis anterior muscles ( $n = 5$  mice, 10 muscles total) were analyzed by rheometry (horizontal line indicates the mean). **(D)** Gel surface protein density did not differ significantly on PEG hydrogels of different rigidities ( $E$ ;  $P > 0.05$ ) and was  $7.6 \text{ ng}/\text{cm}^2 \pm 1.0 \text{ ng}/\text{cm}^2$  ( $n \geq 4$ ). **(E)** Scheme of Baxter algorithm analysis of time-lapse videos. Hydrogel arrays with hundreds of microwells containing single MuSCs were followed by time-lapse microscopy for 3 days. Videos were automatically processed and analyzed (SOM). Scale bar, 100  $\mu\text{m}$ . **(F)** Single MuSC (black data points) velocity on pliant or rigid culture substrates. Circles denote mean velocity  $\pm$  SD ( $P < 0.0001$ ). **(G)** Change in total MuSC number on soft (top plot) or stiff (bottom plot) substrates during time-lapse acquisition. Deaths (X) and divisions (O) are shown, and colors designate five cell generations (G1 to G5). The proportion of cells in each generation at all time points is shown. Cell number is normalized to a starting population of 100 single MuSCs.

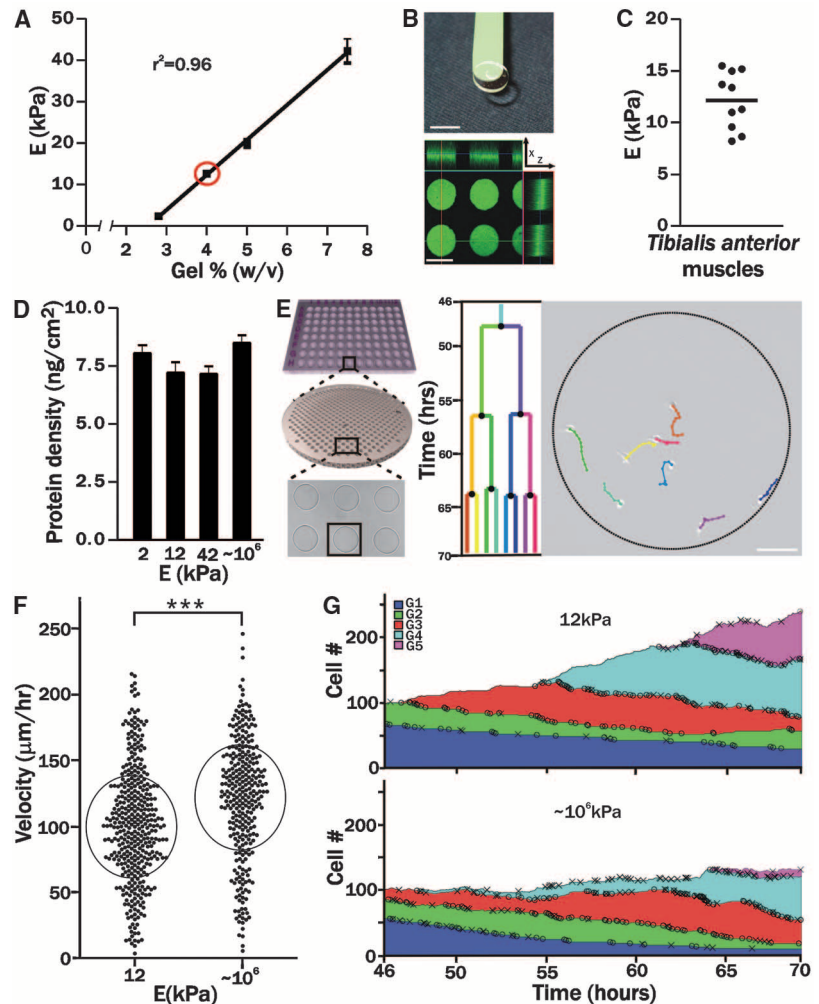
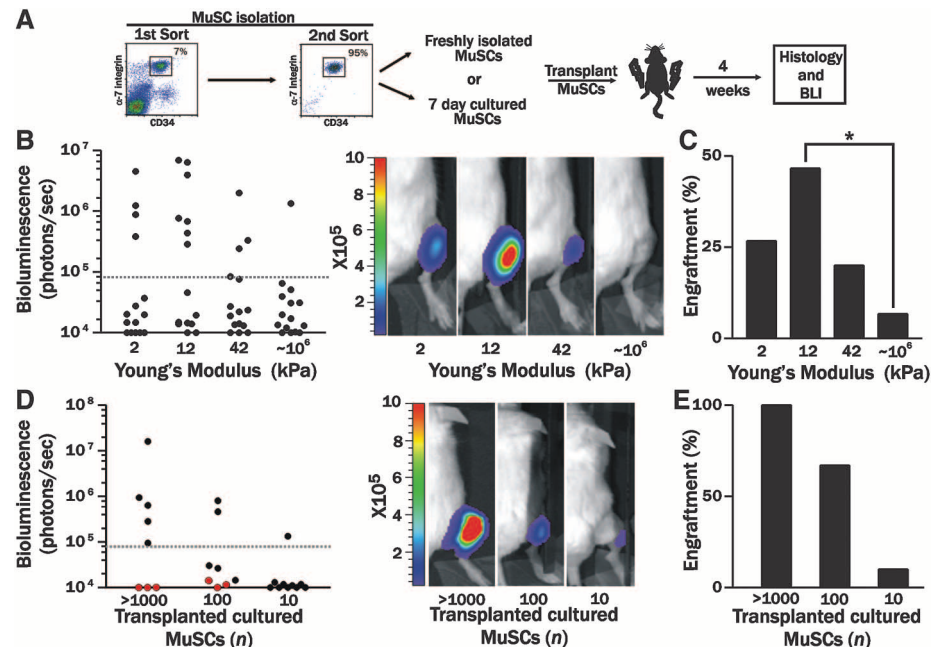


**Fig. 2.** Cultured MuSC engraftment is modulated by substrate elasticity. **(A)** Scheme of *in vivo* transplantation experiments. **(B)** Scatter graph of BLI values of recipient mice 1 month after transplantation with 100 GFP/*Fluc* MuSCs after 7-day culture on substrates of varying stiffness (left;  $n = 15$ ). Representative bioluminescence images of mice transplanted with each culture condition are shown (right; photons  $\text{s}^{-1} \text{cm}^{-2} \text{sr}^{-1}$ ). **(C)** Percentage of mice from each experimental condition that had a BLI value above the engraftment threshold. Fisher's exact test  $P < 0.05$ . **(D)** Scatter graph of BLI values of recipient mice 1 month after transplantation with different numbers of *Fluc* MuSCs cultured for 7 days on either hydrogel (black) or plastic (red). Representative bioluminescence images of mice transplanted with each culture condition are shown (right; photons  $\text{s}^{-1} \text{cm}^{-2} \text{sr}^{-1}$ ). **(E)** Percentage of total transplanted mice in each experimental condition exhibiting a BLI value above the engraftment threshold.





erase (Fluc) (18) and green fluorescent protein (GFP) and cultured for 7 days. Cells were harvested and counted, and cultured MuSC progeny were transplanted into the tibialis anterior (TA) muscles of immunodeficient mice depleted of endogenous MuSCs by 18 Gy leg-irradiation (15, 19). We assayed donor cell behavior quantitatively over time by noninvasive *in vivo* bioluminescence imaging (BLI) of luciferase activity, which correlates with cell number (Fig. 2A) (7). The engraftment threshold was set as the bioluminescence value corresponding with histological detection of donor-derived myofibers (fig. S10). This *in vivo* functional assay is critical for validating the stemness of cultured MuSCs.

*In vivo* functional assays show that MuSCs cultured on substrates matching the physiological modulus of muscle tissue most potently retain stemness. Hydrogel substrates were tuned to mimic the endogenous *in vivo* mechanical properties of brain, muscle, and cartilage (2, 12, or 42 kPa) compared with polystyrene plastic ( $\sim 10^6$  kPa). In agreement with previous reports (3, 7, 9), we observe markedly reduced engraftment from MuSCs cultured on plastic (Fig. 2B). Strikingly, the highest bioluminescent signals are obtained from mice transplanted with MuSCs cultured on the most compliant hydrogels, whereas both the extent and rate of engraftment are decreased on the stiffest culture substrates (Fig. 2B). Notably, the culture substrate

that recapitulates skeletal muscle elasticity (12 kPa) is the only condition that leads to a statistically significant increase in the percentage of mice with MuSC engraftment compared with tissue culture plastic (Fig. 2C).

To determine the proportion of cultured cells with engraftment potential, we cultured MuSCs for 1 week on either soft or rigid substrates and then performed dilution analysis. None of the mice transplanted with stem cells cultured on a rigid plastic substrate exhibit a BLI signal above the threshold of detection (Fig. 2D, red circles). By contrast, engraftment occurs with 100% frequency when  $\geq 1000$  hydrogel-cultured (12 kPa) stem cells are transplanted (Fig. 2D, black circles), similar to freshly isolated cells (7). Moreover, 10% of mice transplanted with only 10 hydrogel cultured cells exhibit engraftment (Fig. 2E), on par with transplantations of 10 freshly isolated cells (16%) (7).

MuSCs cultured on a substrate that mimics muscle tissue exhibit dynamic proliferative behavior similar to freshly isolated MuSCs when transplanted *in vivo*. Both cell populations undergo a period of extensive proliferation that ultimately plateaus and stabilizes when homeostasis is achieved (Fig. 3A). Histology identifies GFP<sup>+</sup> myofibers resulting from regeneration in mice transplanted with MuSCs that were freshly isolated or cultured on soft substrates (Fig. 3B). Although the engraftment rate of freshly isolated MuSCs (7) and those grown on soft substrates is comparable (Fig. 2C), the extent of engraftment from cultured MuSCs is not as robust as that of freshly isolated cells (Fig. 3A), suggesting that exposure to additional biochemical cues *in vitro* may be required to recapitulate other key niche components necessary for maximal function *in vivo*.

MuSCs cultured on soft substrates can home to their native satellite cell niche upon transplantation into muscle, a defining characteristic of freshly isolated MuSCs (3, 7). MuSCs isolated from mice expressing *LacZ* under the regulation of the *Myf5* promoter (20) were cultured on soft hydrogel and subsequently transplanted into mice. Before harvesting tissues, recipient muscles were damaged with notexin (21), which activates MuSCs and up-regulates expression of the myogenic transcription factor *Myf5* (7, 20). Histological analysis of  $\beta$ -galactosidase ( $\beta$ -gal) staining reveals that, like freshly isolated cells (7), transplanted hydrogel cultured cells expressing *Myf5* are found in the satellite cell niche, beneath the basal lamina and atop myofibers (Fig. 3C).

One of the defining characteristics of stem cells is their ability to make more copies of themselves upon division, or self-renew. Several elegant *in vitro* approaches have provided strong evidence that MuSC asymmetric and symmetric divisions occur in culture, consistent with self-renewal (4, 22–27). Our *in vitro* analysis of MuSC gene expression using MuSCs isolated from a Pax7-ZsGreen transgenic mice (28) suggests that a compliant substrate supports self-renewal. We observe that 32% of doublets (two cells that arose from a single cell division) in compliant microwells

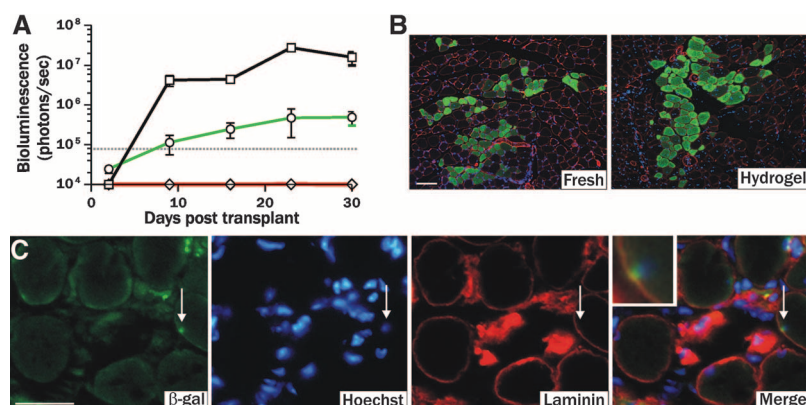


**Fig. 3.** Culture on compliant hydrogel promotes muscle stem cell engraftment and niche repopulation *in vivo*. (A) Engraftment of freshly isolated (black line, squares; 500 cells) and compliant (green line, circles; 1500 cells) or rigid (red line, diamonds; 1500 cells) substrate-cultured MuSCs monitored by BLI for a period of 30 days after transplantation ( $P < 0.05$ ). (B) Immunofluorescence of GFP expression in transverse sections of muscles 1 month after transplantation with freshly isolated (left; 500 transplanted cells) or 1 week compliant hydrogel-cultured MuSCs (right; 2500 transplanted cells). GFP, green; laminin, red; Hoechst, blue. Scale bar, 100  $\mu$ m. (C) Immunohistochemical analysis of transverse muscle tissues 1 month after transplant with compliant substrate-cultured MuSCs. Arrow points to a donor-derived cell in satellite cell position.  $\beta$ -galactosidase, green; laminin, red; Hoechst, blue. Scale bar, 50  $\mu$ m.

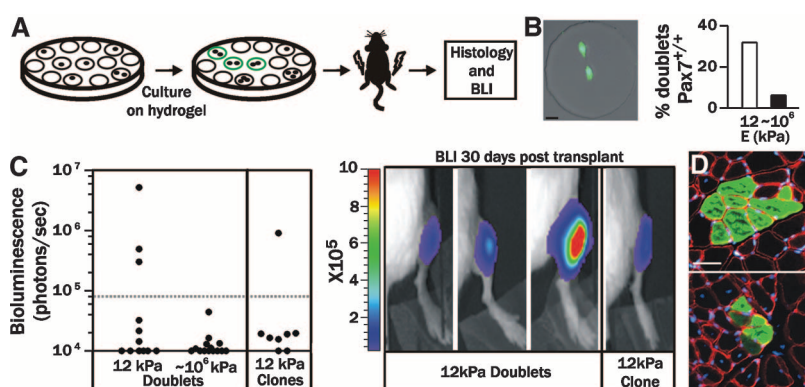


**Fig. 4.** Culture on compliant hydrogel promotes muscle stem cell self-renewal. (A) Scheme of *in vivo* self-renewal assay. (B) Percentage of total doublets exhibiting a Pax7<sup>+/+</sup> gene signature in compliant ( $n = 47$ ) or stiff ( $n = 32$ ) microwells (right). Representative image of a Pax7<sup>+/+</sup> doublet (left). Native Pax7-ZsGreen, green; Hoechst, blue. Scale bar, 20  $\mu$ m. (C) Scatter graph (left) of bioluminescent values from mice transplanted with doublets derived from compliant ( $n = 12$ ) or stiff ( $n = 14$ ) microwells or clones collected from compliant microwells ( $n = 8$ ). Images of mice with bioluminescent values above threshold are shown (right; photons  $s^{-1} cm^{-2} sr^{-1}$ ). (D) Immunohistochemistry of GFP expression in transverse sections of muscles 1 month after transplantation with five MuSC doublets (top, GFP<sup>+</sup> fibers persist  $\sim 13$  mm longitudinally) or a single clone (bottom, fibers persist  $\sim 7$  mm longitudinally) cultured on compliant hydrogel. GFP, green; laminin, red; Hoechst, blue. Scale bar, 100  $\mu$ m.

are positive for the MuSC marker Pax7 (Fig. 4, A and B, and fig. S11). In contrast, only 6% of doublets in plastic microwells have this gene expression pattern, suggesting that a pliant substrate enables MuSC expansion. Although gene expression data are suggestive, an *in vivo* functional assay is necessary to conclude definitively that a self-renewal division event occurred in culture.

We show conclusively that stem cell self-renewal occurs using an *in vivo* functional assay. The transplantation of MuSCs at a population level demonstrates engraftment (Figs. 2 and 3) but does not definitively show that self-renewal divisions occurred in culture, because the population could include nondividing cells that maintained stem cell properties. Accordingly, in this experiment, we plated MuSCs in hydrogel microwell arrays and obtained images immediately after plating and 2 to 3 days after culturing to identify microwells that contained only one doublet. Doublets from 5 microwells were picked and pooled using a micromanipulator, and 10 cells total were transplanted per mouse (Fig. 4A). A detectable BLI signal indicates engraftment resulting from a self-renewal division event that must have occurred in at least one of the five transplanted doublets. Notably, 25% (3 of 12) of mice transplanted with doublets cultured on soft substrates demonstrate detectable engraftment (Fig. 4C) and contribution to regenerating myofibers (Fig. 4D, top), providing *in vivo* functional evidence that MuSC self-renewal division events occur in culture on pliant substrates. In contrast, doublets grown on rigid plastic microwells never exhibit engraftment after transplantation (0 of 14) (Fig. 4C), indicating that their regenerative potential is rapidly lost.

MuSC self-renewal on pliant hydrogel occurs even after multiple divisions. We transplanted clones that arose from a single cell that underwent 3 to 5 divisions. Remarkably, 12% (1 of 8) of mice transplanted with a single clone show engraftment, demonstrating that MuSC self-renewal capacity is retained on pliant substrates even after multiple divisions (Fig. 4, C and D, bottom).

Here, we provide insight into the potency of tissue rigidity, a biophysical property of the skeletal muscle microenvironment, on stem cell fate regulation. Using a single-cell tracking algorithm to interrogate MuSC behaviors at the single-cell level, we demonstrate that soft substrates enhance MuSC survival, prevent differentiation, and promote stemness. Functional assays in mice demonstrate conclusively that pliant substrates permit MuSC self-renewal in culture. Although the underlying mechanisms remain to be elucidated, we hypothesize that decreased rigidity preserves stemness by altering cell shape, resulting in cytoskeletal rearrangements and altered signaling, as shown for cell lines (16). Despite the remarkable retention of stemness in response to a single parameter, rigidity, we anticipate further enhancement of stemness through incorporation of additional biochemical cues into our reductionist platform. Studies employing biomimetic culture platforms, such as described here for MuSCs, will broadly

affect stem cell studies by facilitating *in vitro* propagation while maintaining stemness and the capacity to regenerate tissues, a critical step toward the development of cell-based therapies. As an alternative to embryonic stem cells and iPS cells that must be directed toward a differentiated fate, our approach exploits the existence of native stem cells within tissues that have a well-defined tissue-specific identity.

#### References and Notes

1. D. D. Cornelison, M. S. Filla, H. M. Stanley, A. C. Rapraeger, B. B. Olwin, *Dev. Biol.* **239**, 79 (2001).
2. S. Fukuda *et al.*, *Exp. Cell Res.* **296**, 245 (2004).
3. D. Montarras *et al.*, *Science* **309**, 2064 (2005).
4. S. Kuang, K. Kuroda, F. Le Grand, M. A. Rudnicki, *Cell* **129**, 999 (2007).
5. M. Cerletti *et al.*, *Cell* **134**, 37 (2008).
6. C. A. Collins *et al.*, *Cell* **122**, 289 (2005).
7. A. Sacco, R. Doyonnas, P. Kraft, S. Vitorovic, H. M. Blau, *Nature* **456**, 502 (2008).
8. R. I. Sherwood *et al.*, *Cell* **119**, 543 (2004).
9. Z. Qu-Petersen *et al.*, *J. Cell Biol.* **157**, 851 (2002).
10. E. Gussoni *et al.*, *Nature* **356**, 435 (1992).
11. M. P. Lutolf, P. M. Gilbert, H. M. Blau, *Nature* **462**, 433 (2009).
12. A. J. Engler, S. Sen, H. L. Sweeney, D. E. Discher, *Cell* **126**, 677 (2006).
13. W. D. Callister, *Fundamentals of Materials Science and Engineering: An Interactive E-Text* (Wiley, Somerset, NJ, ed. 5, 2000).
14. M. P. Lutolf, R. Doyonnas, K. L. Havenstrite, K. Kolekar, H. M. Blau, *Integr. Biol.* **1**, 59 (2009).
15. L. Heslop, J. E. Morgan, T. A. Partridge, *J. Cell Sci.* **113**, 2299 (2000).
16. R. J. Pelham Jr., Y. Wang, *Proc. Natl. Acad. Sci. U.S.A.* **94**, 13661 (1997).
17. T. A. Partridge, in *Basic Cell Culture Protocols*, J. W. Pollard, J. M. Walker, Eds. (Humana Press, Totowa, NJ, 1997), vol. 75, pp. 131–144.
18. Y. A. Cao *et al.*, *Proc. Natl. Acad. Sci. U.S.A.* **101**, 221 (2004).
19. S. Wakeford, D. J. Watt, T. A. Partridge, *Muscle Nerve* **14**, 42 (1991).
20. S. Tajbakhsh *et al.*, *Dev. Dyn.* **206**, 291 (1996).
21. J. B. Harris, M. A. Johnson, *Clin. Exp. Pharmacol. Physiol.* **5**, 587 (1978).
22. R. Abou-Khalil *et al.*, *Cell Stem Cell* **5**, 298 (2009).
23. V. Shinin, B. Gayraud-Morel, D. Gomès, S. Tajbakhsh, *Nat. Cell Biol.* **8**, 677 (2006).
24. M. J. Conboy, A. O. Karasov, T. A. Rando, *PLoS Biol.* **5**, e102 (2007).
25. I. M. Conboy, T. A. Rando, *Dev. Cell* **3**, 397 (2002).
26. F. Le Grand, A. E. Jones, V. Seale, A. Scimè, M. A. Rudnicki, *Cell Stem Cell* **4**, 535 (2009).
27. P. S. Zammit *et al.*, *J. Cell Biol.* **166**, 347 (2004).
28. D. Bosnakovski *et al.*, *Stem Cells* **26**, 3194 (2008).
29. We thank K. Kolekar, R. Tran, IBM Almaden, the Stanford Center for Innovation in In-Vivo Imaging, and the Stanford Shared FACS Facility core facilities for technical support; J. Sly, R. D. Miller, S. Kobal, S. Gobaa, R. Doyonnas, and A. Barron for valuable discussions; and F. Rossi and M. Kyba for providing alpha-7 integrin antibody and Pax7-ZsGreen mice, respectively. This work was financially supported by PHS CA09151 and CIRM TG2-01159 (P.M.G.); Leukemia and Lymphoma Society Fellow and European Young Investigator Award (M.P.L.); NSF and NIH Training Grant 2 T32 HD007249 (K.H.); Muscular Dystrophy Association (MDA) grant 4063 (A.S.); EPFL Excellence Scholarship and the Swiss Study Foundation (N.A.L.); John och Karin Engbloms Stipendiefond (K.E.G.M.); Bio X Undergraduate Research Award and Howard Hughes Medical Institute grant 52005886 (N.K.N.); and NIH grants HL096113, AG009521, AG020961, U01 HL100397, JDRF 34-2008-623, MDA grant 4320, LLS grant TR6025-09, CIRM grant RT1-01001, Stanford Bio-X Award IIP3-34, and the Baxter Foundation (H.M.B.).

#### Supporting Online Material

www.sciencemag.org/cgi/content/full/science.1191035/DC1  
Materials and Methods

Figs. S1 to S11

References

Movie S1

16 April 2010; accepted 30 June 2010

Published online 15 July 2010;

10.1126/science.1191035

Include this information when citing this paper.

## Optimally Interacting Minds

Bahador Bahrami,<sup>1,2,3\*</sup> Karsten Olsen,<sup>3</sup> Peter E. Latham,<sup>4</sup> Andreas Roepstorff,<sup>3</sup> Geraint Rees,<sup>1,2</sup> Chris D. Frith<sup>2,3</sup>

In everyday life, many people believe that two heads are better than one. Our ability to solve problems together appears to be fundamental to the current dominance and future survival of the human species. But are two heads really better than one? We addressed this question in the context of a collective low-level perceptual decision-making task. For two observers of nearly equal visual sensitivity, two heads were definitely better than one, provided they were given the opportunity to communicate freely, even in the absence of any feedback about decision outcomes. But for observers with very different visual sensitivities, two heads were actually worse than the better one. These seemingly discrepant patterns of group behavior can be explained by a model in which two heads are Bayes optimal under the assumption that individuals accurately communicate their level of confidence on every trial.

To come to an optimal joint decision, individuals must share information with each other and, importantly, weigh that information by its reliability (1, 2). It has been well established that isolated individuals can accurately weigh information when combining different sources of sensory information (3–5). Little is known, however, about how, or even whether, two

individuals can accurately combine information that they communicate with each other. To investigate this issue, we examined the behavior of pairs of individuals in a simple perceptual decision task, and we asked how signals from the same sensory modality (vision) in the brains of two different individuals could be combined through social interaction.